ARTICLE IN PRESS

Inorganica Chimica Acta xxx (2015) xxx–xxx

Contents lists available at ScienceDirect

Inorganica Chimica Acta

journal homepage: www.elsevier.com/locate/ica

Titanium, zirconium and vanadium complexes of 2-(benzimidazolyl, benzothiazolyl, and benzoxazolyl) pyridine as catalyst precursors for ethylene polymerization

Hamdi Ali Elagab, Helmut G. Alt *

Laboratorium für Anorganische Chemie, Universität Bayreuth, Postfach 10 12 51, D-95440 Bayreuth, Germany

ARTICLE INFO

Article history:
Received 25 January 2015
Received in revised form 14 March 2015
Accepted 17 March 2015
Available online xxxx

Dedicated to Professor Dr. Uwe Rosenthal on the occasion of his 65th birthday (April 23).

Keywords:
2-(Benzimidazolyl, benzothiazolyl, benzoxazolyl) pyridine complexes
Titanium, zirconium, vanadium
Homogeneous ethylene polymerization
Structure–property-relationships

ABSTRACT

Dissymmetric chelating complexes of Ti, Zr and V with 2-(benzimidazolyl, benzothiazolyl, and benzoxazolyl) pyridine ligands were synthesized and characterized. After activation with methylalumoxane (MAO) in solution, these complexes could be applied as ethylene polymerization catalysts. Their activities depend on the metal and the substituents at the pyridine ring and the heterocycle. Structure–property-relationship studies revealed that the titanium and vanadium catalyst systems showed higher polymerization activities than the zirconium analogues. The benzoxazolyl moiety containing vanadium complex **29**, with a methyl substituent in the 6-membered ring in meta position to the nitrogen atom in the 5-membered ring, and an unsubstituted pyridine ring showed the highest activity (1154.8 kg PE/mol cat h). The produced polyethylenes exhibited high molecular weights and broad molecular weight distributions. Obviously different active sites are generated in the course of these polymerization reactions.

1. Introduction

Recently we reported the synthesis and the characterization of 2,6-bis-(benzimidazolyl, benzothiazolyl, and benzoxazolyl) benzene complexes with the metals, titanium, zirconium and vanadium [1,2]. These complexes could be activated with methylalumoxane (MAO) in solution and be applied as catalysts for homogeneous ethylene polymerization. Now we modified these ligands in a way that we removed one heterocyclic moiety and the bridging unit and instead placed a pyridyl substituent on the carbon atom of the heterocyclic 5-membered ring.

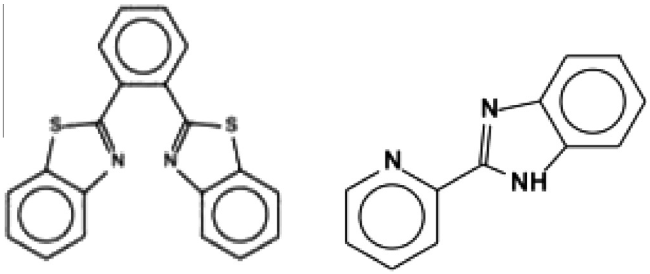

2,6-Bis-(benzimidazolyl) [3–7], 2,6-bis(benzothiazolyl) pyridine [8] and 2,6-bis(benzoxazolyl) pyridine [9,10] already have been reported as ligands for several transition metals in order to investigate the complexes for their structures and properties. In polyolefin chemistry, an increasing interest has been focused on the development and design of homogeneous transition metal catalysts as a result of an increasing demand for polyethylene [11–15 and references therein]. So far, vanadium complexes with bis-(benzimidazole) amine as tridentate [N, N, N] ligands were described as active ethylene polymerization catalysts after activation with alkylaluminum compounds [16]. 2,6-Bis(2-benzimidazolyl) pyridine zirconium dichloride/MAO polymerizes methylacrylate [17]. Now we report the first titanium(IV), zirconium(IV) and vanadium(III) complexes with the title ligands together with their use as catalysts for ethylene polymerization after activation with methylalumoxane (MAO).

2. Results and discussion

2.1. Synthesis of the pyridine derivatives 1–8

The compounds **1**–**8** were synthesized according to Scheme 1 via the polyphosphoric acid method [18]. Condensation reactions of 2-pyridine carboxylic acid, or 6-methyl-2-pyridine carboxylic

---

* Corresponding author. Tel.: +49 921 43864.
E-mail address: helmut.alt@uni-bayreuth.de (H.G. Alt).

http://dx.doi.org/10.1016/j.ica.2015.03.021
0020-1693/© 2015 Elsevier B.V. All rights reserved.

Please cite this article in press as: H.A. Elagab, H.G. Alt, Inorg. Chim. Acta (2015), http://dx.doi.org/10.1016/j.ica.2015.03.021

acid with 2-aminothiophenol, o-phenylene diamine, 3-methyl-o-phenylene, diamine, 2-amino-4-methylphenol, and 2-amino-5-methylphenol were performed. The products were obtained in high yields (⩾85%). The Phillip's modified method [19,20] failed to give any of the desired products.

2.2. Synthesis of the coordination compounds

The complexes **9**–**32** were synthesized according to Scheme 2 by mixing the organic compounds and the corresponding metal salt (VCl_3) or the tetrahydrofuran adducts of zirconium and titanium tetrachloride in an appropriate solvent and stirring the mixture over night. The products were obtained in very good yields.

2.3. Characterization

2.3.1. ^1H and ^{13}C NMR spectroscopy

The compounds **1**–**8** were characterized by ^1H NMR and ^{13}C NMR spectroscopy. The ^1H NMR spectrum of compound **3** (Fig. 1) shows seven sets of signals. The broad signal with low intensity at $\delta = 9.88$ ppm belongs to the NH proton, a doublet at $\delta = 8.25$ ppm [1H, $^3J_{H,H} = 7.5$ Hz] can be assigned to the pyridine ring proton H3, a virtual triplet at $\delta = 7.82$ ppm [1H, $^3J_{H,H} = 7.5$ Hz] to H2. The multiplets at $\delta = 7.72$–7.68 and 7.27–7.25 ppm belong to an AA′BB′ spin system and can be assigned to the phenyl protons H4, H7 and H5, H6. H1 appears at $\delta = 7.38$ ppm [d, 1H, $^3J_{H,H} = 7.5$ Hz]. The methyl protons are found as a singlet at $\delta = 2.58$ ppm.

The ^{13}C NMR spectrum of compound **3** (Fig. 2) shows ten signals. The signal at $\delta = 159.1$ ppm corresponds to C1, the signal at $\delta = 150.2$ ppm to C5. The signals at $\delta = 146.0$ and 138.6 ppm can be assigned to C12 and C3. The signal at $\delta = 137.2$ ppm arises from the two carbon atoms of the phenyl ring (C6, C11). The carbon atom C2 of the pyridine ring appears at $\delta = 125.9$ ppm, C8 and C9 at $\delta = 124.4$ ppm. The signal at $\delta = 120.1$ ppm corresponds to C4, while C7 and C10 are observed at $\delta = 115.9$ ppm. At $\delta = 24.7$ ppm, the methyl carbon atom (C13) can be detected.

Complexes **9**–**32** were characterized by ^1H NMR and ^{13}C NMR spectroscopy. The ^1H NMR spectrum of complex **19** (Fig. 3) shows six resonance signals: the super imposed doublets at $\delta = 8.84$ ppm correspond to H1 and H4. The virtual triplets at $\delta = 8.19$ and 7.68 ppm [$^3J_{H,H} = 7.5$ Hz] belong to H3 and H2. H5 and H6 form an AB pattern at $\delta = 7.62$ and 7.35 ppm [$^3J_{H,H} = 8.5$ Hz], and H7 a singlet at $\delta = 7.56$ ppm. The protons of the methyl group can be observed at $\delta = 2.02$ ppm.

The ^{13}C NMR spectrum of complex **19** (Fig. 4) shows 13 resonance signals: the signal at $\delta = 151.1$ ppm can be assigned to C12. C1 appears at $\delta = 147.2$ ppm while the signals at $\delta = 142.6$, 139.0 and 137.2 ppm belong to C5, C11 and C6. The signals at $\delta = 133.6$ and 130.5 ppm derive from C3 and C8. The signals at $\delta = 128.7$ and 128.1 ppm were assigned to C9 and C2. Further signals at $\delta = 124.6$, 114.6, and 114.3 ppm belong to C7, C4 and C10. The methyl carbon (C13) signal is found at $\delta = 21.9$ ppm.

2.3.2. Mass spectrometry

The compounds **1**–**8**, in addition to their ^1H NMR and ^{13}C NMR spectra, were characterized by mass spectrometry. The mass spectrum of compound **3** shows the molecular ion at $m/z = 209$. The ion resulting from the loss of a methyl group is represented by $m/z = 194$ (the full fragmentation pattern is shown in Fig. 5).

In addition to their NMR spectra, the complexes **9**–**32** were characterized by mass spectroscopy. The mass spectrum of complex **19** (Fig. 6) shows an incomplete fragmentation pattern. The reason is the fact that the n-donor bonds in the complex do not survive the ionization process. A molecular ion cannot be observed. The peak at $m/z = 209$ can be assigned to the free ligand.

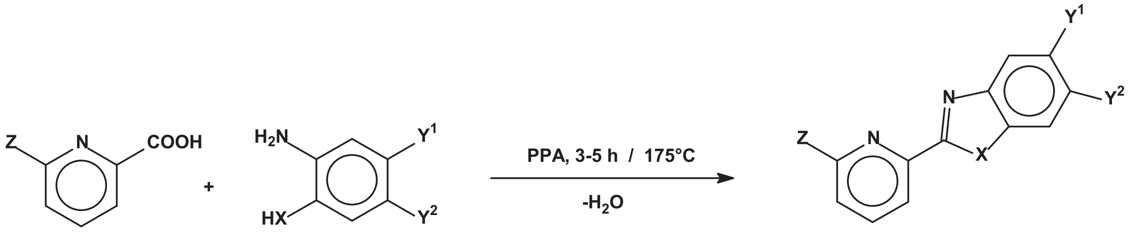

No.	X	Y^1	Y^2	Z
1	S	H	H	H
2	NH	H	H	H
3	NH	H	H	CH_3
4	NH	CH_3	H	H
5	NH	Cl	H	H
6	O	H	H	H
7	O	CH_3	H	H
8	O	H	CH_3	H

Scheme 1. Synthesis of the potential ligand **1**–**8**.

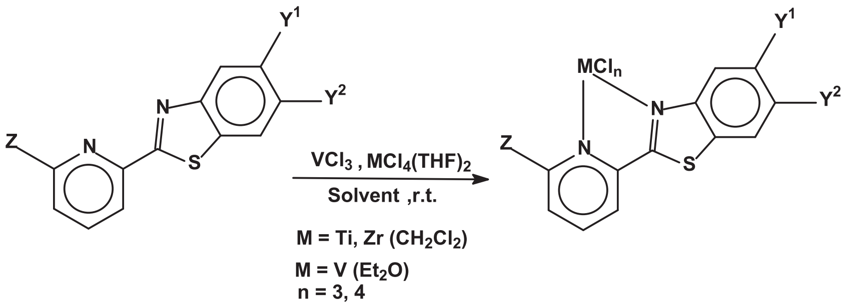

Complex	X	Y^1	Y^2	Z	M
9	S	H	H	H	Ti
10	S	H	H	H	Zr
11	S	H	H	H	V
12	NH	H	H	H	Ti
13	NH	H	H	H	Zr
14	NH	H	H	H	V
15	NH	H	H	CH_3	Ti
16	NH	H	H	CH_3	Zr
17	NH	H	H	CH_3	V
18	NH	CH_3	H	H	Ti
19	NH	CH_3	H	H	Zr
20	NH	CH_3	H	H	V
21	NH	Cl	H	H	Ti
22	NH	Cl	H	H	Zr
23	NH	Cl	H	H	V
24	O	H	H	H	Ti
25	O	H	H	H	Zr
26	O	H	H	H	V
27	O	CH_3	H	H	Ti
28	O	CH_3	H	H	Zr
29	O	CH_3	H	H	V
30	O	H	CH_3	H	Ti
31	O	H	CH_3	H	Zr
32	O	H	CH_3	H	V

Scheme 2. The synthesized transition metal complexes **9**–**32**.

2.4. Polymerization results

All coordination compounds were activated with MAO. The mechanism should be the same as it was proposed for the activation of metallocene [21,22] and 2,6-bis(imino) pyridine iron(II) [23] catalyst precursors (see Table 1).

The titanium and zirconium complexes of 2-(benzimidazolyl) pyridine, 2-(benzothiazolyl) pyridine and 2-(benzoxazolyl) pyridine, after activation with MAO, showed catalytic activities for ethylene polymerization reactions. In all cases, the titanium complexes are more active than the zirconium complexes with the same ligand system (Fig. 7). This could be due to the fact that zirconium forms thermodynamically stronger metal carbon bonds and as a consequence kinetics in the various polymerization steps are slowed down. The 2-(benzothiazolyl) pyridine titanium complex **9** showed an activity of 548 kg PE/mol cat h which can be attributed to an extra stabilization of the active centre via a secondary interaction with the sulfur atom.

Please cite this article in press as: H.A. Elagab, H.G. Alt, Inorg. Chim. Acta (2015), http://dx.doi.org/10.1016/j.ica.2015.03.021

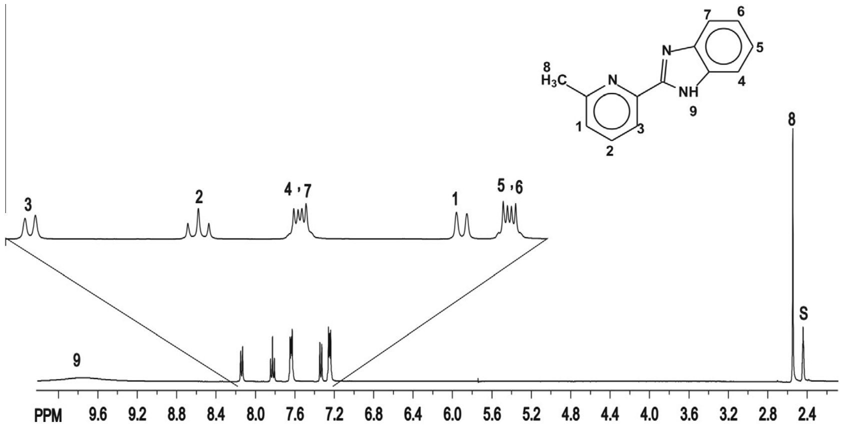

Fig. 1. ^{1}H NMR spectrum of compound **3** in DMSO-d_6.

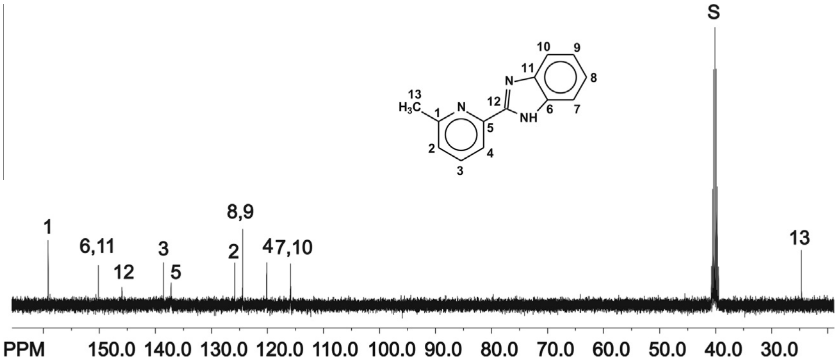

Fig. 2. ^{13}C NMR spectrum of compound **3** in DMSO-d_6.

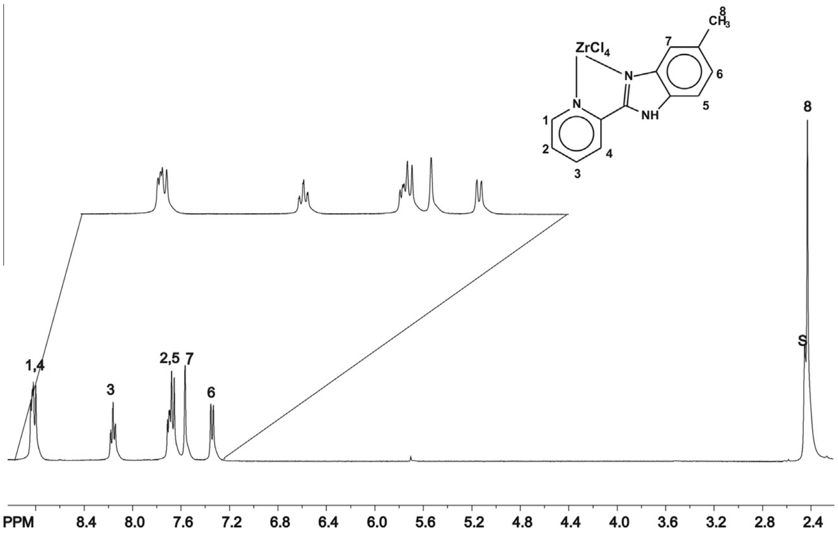

Fig. 3. ^{1}H NMR spectrum of complex **19**.

Titanium complexes of 2-(benzimidazolyl) pyridine (**12**), and 2-(benzoxazolyl) pyridine (**24**) show similar activities (307 and 336 kg PE/mol cat h) most probably due to the comparable sizes and electronegativities of the hetero atoms (N, O). The same behavior was observed for the zirconium complexes **13** and **25** (126 and 127 kg PE/mol cat h) of the same ligand systems (Fig. 7).

In all cases methyl substituted 2-(benzoxazolyl) pyridine titanium complexes showed lower activities compared to the unsubstituted derivatives (Fig. 8). The position of the methyl group influences the activity via electronic and/or steric effects but also because of the interaction catalyst cation/MAO anion. The catalyst system **27**/MAO with a methyl substituent *meta* to the imino nitrogen atom showed an activity of 297 [kg PE/mol cat h]. The catalyst system **31**/MAO with a methyl substituent *para* to the imino nitrogen atom gave an activity of 275 [kg PE/mol cat h] while the unsubstituted complex **24/MAO** reached an activity of 336 [kg PE/mol cat h].

Please cite this article in press as: H.A. Elagab, H.G. Alt, Inorg. Chim. Acta (2015), http://dx.doi.org/10.1016/j.ica.2015.03.021

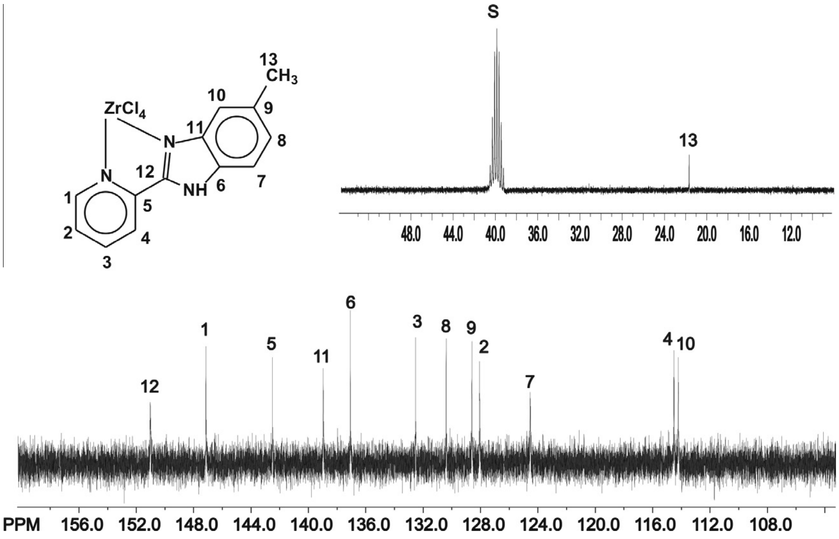

Fig. 4. ^{13}C NMR spectrum of complex **19**.

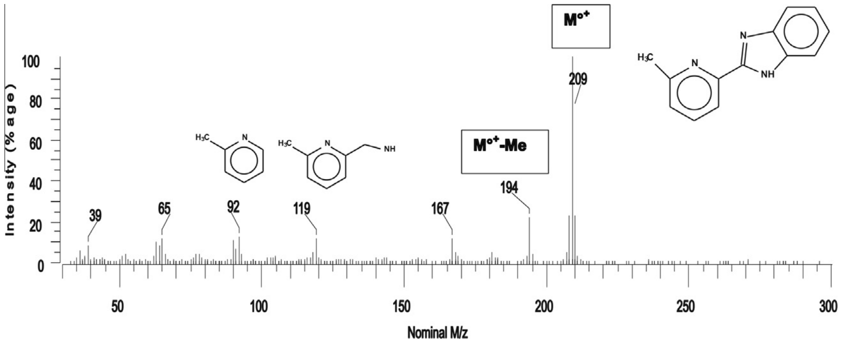

Fig. 5. Mass spectrum of compound **3**.

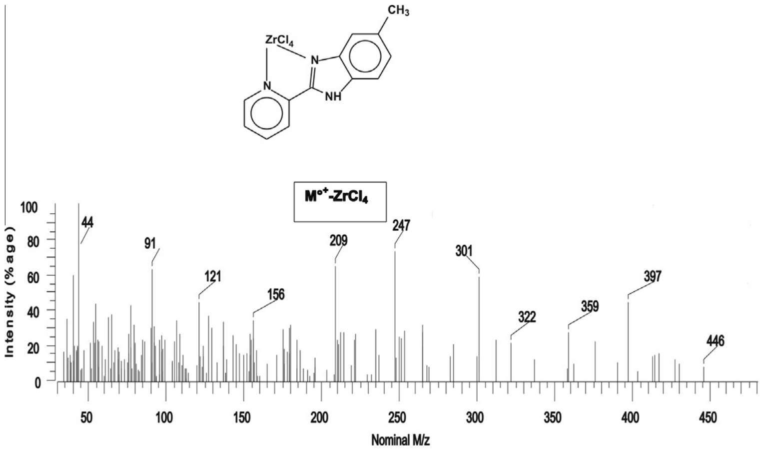

Fig. 6. Mass spectrum of complex **1**.

The investigation of the ethylene polymerization activities of 2-(benzimidazolyl) pyridine and 2-(benzoxazolyl) pyridine zirconium complexes revealed that the unsubstituted complexes showed higher activities than those with methyl substituents on the phenyl ring, which gave the same activities regardless to the position of the substituent. In the series of zirconium complexes, the 2-(benzimidazolyl) pyridine complex **16** with a methyl substituent in the ortho position of the pyridine ring showed the highest activity (192 kg PE/mol cat h) probably because of the increasing steric bulk around the active center (Fig. 9) keeping the MAO counter anion at further distance. Complex **22** with a chloro substituent *meta* to the imino nitrogen showed a higher activity than the unsubstituted complex **13** (126 kg PE/mol cat h) most probably for electronic reasons increasing the Lewis acidity of the active center.

Also the vanadium complexes of 2-(benzimidazolyl) pyridine, 2-(benzothiazolyl) pyridine, and 2-(benzoxazolyl) pyridine, after activation with MAO, showed catalytic activities in ethylene polymerization reactions. The activities show the following trend: 2-(benzoxazolyl) pyridine vanadium complexes are more active than 2-(benzothiazolyl) pyridine complexes and 2-(benzimidazolyl) pyridine complexes; i.e., the activities of these vanadium complexes with such ligands are greatly influenced by different hetero atoms (Fig. 10). Surprisingly the benzoxazolyl derivative **26** showed the best activity obviously because of the dominating -I effect of oxygen on the active center.

The position and the type of the substituent have a strong influence on the activities of 2-(benzimidazolyl) pyridine and 2-(benzoxazolyl) pyridine vanadium complexes (Fig. 11). Complex **17** with a methyl substituent in the ortho position of the pyridine ring shows an activity of 295.4 [kg PE/mol cat h], complex **20** with a methyl substituent at the meta position of the phenylidene ring 278.2 [kg PE/mol cat h] while the chloro (*meta* to the imino nitrogen) substituted complex **23** reaches an activity of only 109 [kg PE/mol cat h] (Fig. 11). It is obvious that electron donating groups on those positions increase the activities of the catalysts while electron withdrawing groups reduce their activities. In an analogous manner the activities of the vanadium 2-(benzoxazolyl) pyridine complexes **29** and **32** with methyl substituents either at the *meta* or *para* position to the imino nitrogen show activities of 1154.8 [kg PE/mol cat h] and 148.6 [kg PE/mol cat h], respectively. This enormous difference of activities could be due to different catalyst cation/MAO anion interactions caused by steric differences.

GPC analyses of representative samples revealed that the catalyst systems produced polyethylenes with very high molecular weights associated with broad molecular weight distributions. For example, the catalyst system **12**/MAO produced polyethylene with a molecular weight of Mw = 1.76 × 10^6 g/mol and a polydispersity PD = 4.4. The catalyst system **9**/MAO produced polyethylene with a molecular weight of Mw = 1.6 × 10^6 g/mol and a polydispersity PD = 5.7, while the polyethylene produced with the catalyst system **20**/MAO shows a molecular weight of Mw = 146 × 10^6 g/mol and a polydispersity PD = 4.5. The high molecular weight resins suggest that the rate of propagation reactions [24,25] are much faster than the rate of termination. The comparatively broad molecular weight distributions are unusual for single site catalysts. Obviously several active sites are generated in the course of the polymerization reaction. This could result from different interactions of the Lewis acidic sites of MAO and the Lewis basic character of the hetero atoms in the catalyst complex giving adducts of different symmetry. In case of the bis(benzimidazolyl)benzene zirconiumtetra-chloride complex much higher PD values (PD = 223) were obtained [26] and we assume that the Lewis basicity of the hetero atoms in the catalyst determines the magnitude of this effect.

Table 1
Ethylene polymerization activities of the complexes **9**–**32**.

Catalyst no.	Activity [kg PE/mol cat h]
9	548.1
10	56.1
11	286.3
12	306.9
13	126.3
14	164.3
15	221.5
16	191.7
17	295.4
18	37.5
19	47.1
20	278.2
21	289.8
22	160.7
23	109.3
24	336.0
25	127.1
26	634.5
27	297.0
28	54.9
29	1154.8
30	275.9
31	47.7
32	148.6

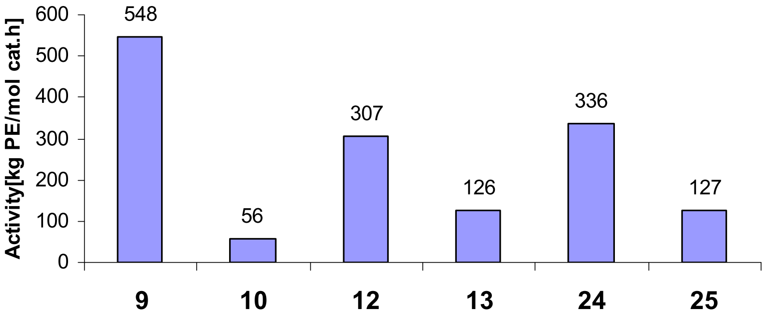

Fig. 7. Polymerization activities of 2-(benzothiazolyl, benzimidazolyl, and benzoxazolyl)-pyridine titanium (**9**, **12**, **24**) and zirconium (**10**, **13**, **25**) complexes.

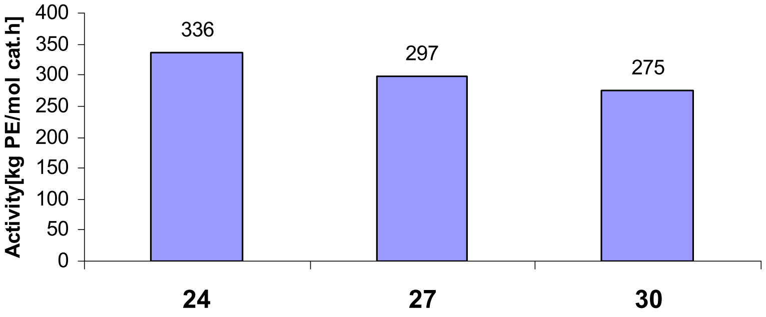

Fig. 8. Effect of substituents on the activities of the 2-(benzoxazolyl) pyridine titanium complexes **24**, **27**, and **30**.

Please cite this article in press as: H.A. Elagab, H.G. Alt, Inorg. Chim. Acta (2015), http://dx.doi.org/10.1016/j.ica.2015.03.021

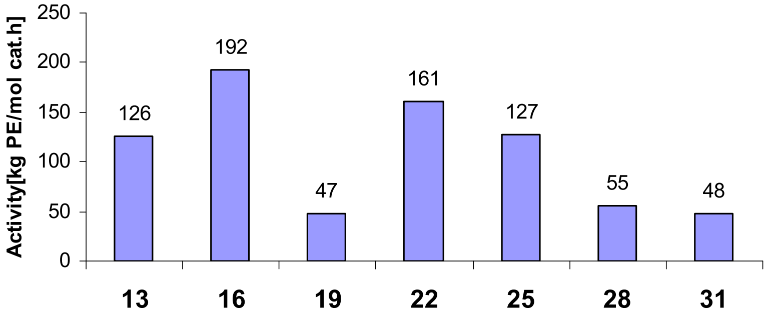

Fig. 9. Effect of the substituent position and type on the activities of 2-(benzimidazolyl, benzoxazolyl) pyridine zirconium complexes.

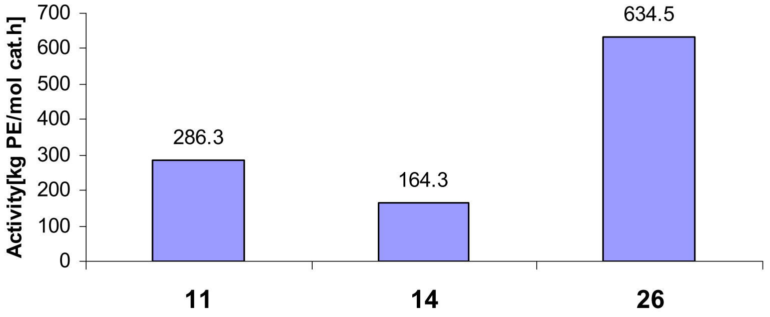

Fig. 10. Effect of the hetero atoms on the activities of the vanadium complexes **11**.

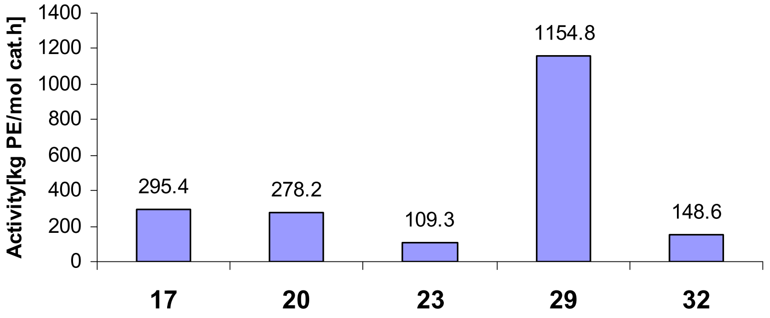

Fig. 11. Effect of substituent position and type on the activities of 2-(benzimidazolyl, benzoxazolyl) pyridine vanadium complexes.

Table 2
Thermal analysis data for representative polymer samples produced with complexes **18**, **19**, **24**, **29**.

Complex no.	T_m (°C)	T_x (°C)	α
18	138.4	120.5	15.4
19	141.5	119.6	31
24	137.4	115.1	38
29	136.2	120.5	25.2

T_m = melting temperature, T_x = crystallization temperature, α = degree of crystallinity.

DSC measurements (see Table 2) showed that the catalyst systems produced HDPE with a high degree of crystallinity. For example, the melting and crystallization temperatures of the polyethylene produced with the catalyst system **19**/MAO was 141.5 and 119.6 °C and the degree of crystallinity α = 31% (see Fig. 12).

3. Experimental

All experimental work was routinely carried out using Schlenk technique unless otherwise stated. Anhydrous and purified argon was used as inert gas. n-Pentane, diethyl ether, toluene and tetrahydrofuran were purified by distillation over Na/K alloy. Diethyl ether was additionally distilled over lithium aluminum hydride. Methylene chloride was dried with phosphorus pentoxide and in a different run with calcium hydride. Methanol and ethanol were dried over molecular sieves. Deuterated solvents ($CDCl_3$, DMSO) for NMR spectroscopy were stored over molecular sieves (3 Å).

Methylalumoxane (30% in toluene) was purchased from Crompton (Bergkamen) and Albemarle (Baton Rouge, USA/Louvain – La Neuve, Belgium). Ethylene (3.0) and argon (4.8/5.0) were supplied by Rießner Company (Lichtenfels). All other starting materials were commercially available and were used without further purification. The titanium and zirconium adducts were synthesized via published procedures [27].

3.1. NMR spectroscopy

The spectrometers Varian Inova 300/400 M Hz and Bruker ARX 250 were available for recording the NMR spectra. The samples were prepared under inert atmosphere (argon) and routinely recorded at 25 °C. The chemical shifts in the ^{1}H NMR spectra are

Please cite this article in press as: H.A. Elagab, H.G. Alt, Inorg. Chim. Acta (2015), http://dx.doi.org/10.1016/j.ica.2015.03.021

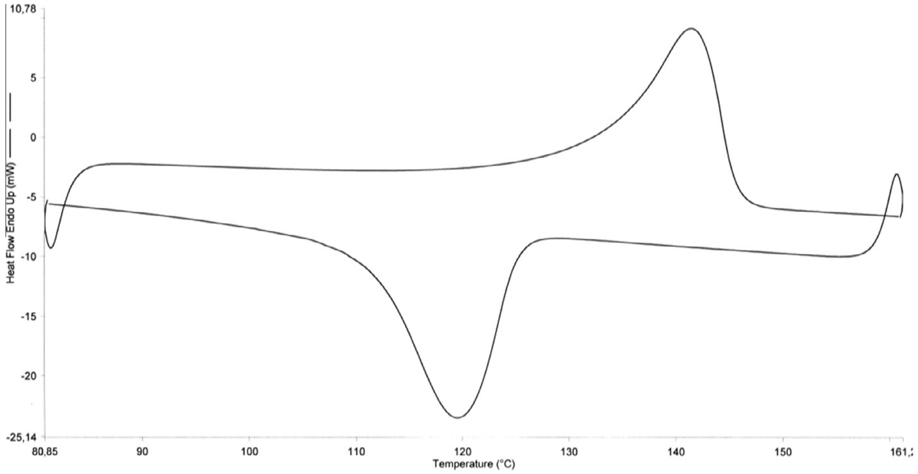

Fig. 12. DSC curves of polyethylene produced with the catalyst system **19/MAO**.

referred to the residual proton signal of the solvent (δ = 7.24 ppm for $CDCl_3$, δ = 2.5 ppm for DMSO) and in ^{13}C NMR spectra to the solvent signal (δ = 77.0 ppm for $CDCl_3$, δ = 39.5 ppm for DMSO).

3.2. Mass spectrometry

Mass spectra were routinely recorded at the Zentrale Analytik of the University of Bayreuth with a VARIAN MAT CH-7 instrument (direct inlet, EI, E = 70 eV) and a VARIAN MAT 8500 spectrometer.

3.3. Gel permeation chromatography (GPC)

GPC measurements were routinely performed by SABIC Company (Riyadh, Saudi Arabia).

3.4. Elemental analysis

Elemental analyses were performed with a VarioEl III CHN instrument. The raw values of the carbon, hydrogen, and nitrogen contents were multiplied with calibration factors (calibration compound: acetamide).

3.5. General procedures for the syntheses of the complexes

*3.5.1. Syntheses of organic compounds **1**–**8***

A diamine compound (0.05 mol) was mixed with a dicarboxylic acid or an acid anhydride (0.025 mol) and the mixture was poured into 50 ml of preheated (100 °C) polyphosphoric acid. The mixture was stirred and heated at 175 °C for 3–5 h. The reaction mixture was then poured in ice cold water and allowed to stand overnight. The precipitate was removed by filtration and washed several times with diluted sodium hydrogen carbonate solution and finally with water. The reaction product was then air dried and weighed. The products were characterized with NMR and mass spectroscopy (Table 4) and representative examples were characterized with elemental analysis (Table 3).

3.5.2. Titanium complexes

To an amount of 0.87 g, (2.6 mmol) $TiCl_4(THF)_2$ in dichloromethane was added 2.6 mmol of the free ligand. The reaction mixture was stirred over night at room temperature. The product was filtered and washed several times with pentane and dried under vacuum and weighed. The products were characterized by NMR and mass spectroscopy (Table 4) and representative examples were characterized with elemental analysis (Table 3).

Table 3
Elemental analysis data for representative free ligands **1**, **2**, **7** and complexes **10**, **14**, **17**, **20**, **24**, **25**, **30**.

Compound no.	Calculated			Found		
	C	H	N	C	H	N
1	78.84	4.61	21.34	78.86	4.58	21.45
2	67.92	3.77	13.21	67.87	3.81	13.16
7	74.28	4.76	13.33	74.32	4.78	13.36
10	32.36	1.80	6.29	32.07	1.78	6.24
14	40.91	2.56	11.93	40.68	2.54	11.86
17	42.62	3.01	11.48	42.16	2.97	11.35
20	42.62	3.01	11.48	42.47	3.14	11.41
24	37.31	2.11	7.25	37.01	2.32	6.99
25	33.57	1.86	6.53	33.93	2.04	6.74
30	39.00	2.50	7.00	39.37	2.66	7.31

3.5.3. Zirconium complexes

To an amount of 0.45 g (1.2 mmol) $ZrCl_4(THF)_2$ in dichloromethane was added 1.2 mmol of the free ligand. The reaction mixture was stirred over night at room temperature. The product was filtered and washed several times with dichloromethane, then with pentane, dried under vacuum and weighed. The products were characterized by NMR and mass spectroscopy (Table 4). Representative examples were characterized with elemental analysis (Table 3).

3.5.4. Vanadium complexes

To an amount of 0.41 g (2.6 mmol) VCl_3 in ether was added 2.6 mmol of the free ligand. The reaction mixture was stirred over night at room temperature. The product was filtered and washed several times with ether and pentane, dried under vacuum and weighed. The products were characterized by mass spectroscopy and representative examples were characterized with elemental analysis (Table 3).

3.6. Polymerization of ethylene in a 1 L Büchi autoclave

An amount of 2–5 mg of the desired complex was suspended in 5 ml of toluene. Methylalumoxane (30% in toluene) was added resulting in an immediate color change. The mixture was added to a 1 L Schlenk flask filled with 250 ml n-pentane. This mixture was transferred to a 1 L Büchi laboratory autoclave under inert atmosphere and thermostated. An ethylene pressure of 10 bar was applied for 1 h. The polymer was filtered over a frit, washed with diluted hydrochloric acid, water, and acetone, and finally dried in vacuo.

Please cite this article in press as: H.A. Elagab, H.G. Alt, Inorg. Chim. Acta (2015), http://dx.doi.org/10.1016/j.ica.2015.03.021

Table 4
NMR and mass spectroscopic data for the free ligands **1**–**8** and complexes **9**–**32**.

Compound no.	^{1}H NMR δ [ppm]	^{13}C NMR δ [ppm]	Mass m/z (%)
1	8.69(d,1H), 8.29(d,1H), 7.95(t,1H), 7.59–7.57(m,2H), 7.48(t,1H), 7.19–7.17(m,2H)	151.3, 150.0, 149.1, 138.2, 125.4, 123.2, 122.1	195 M$^{\cdot+}$ (100)
2	8.24(d,1H), 7.82(t,1H), 7.72–7.68(m,2H), 7.38(d,1H), 7.27–7.25(m,2H), 2.58(s,3H,CH$_3$)	159.1, 150.2, 145.9, 138.6, 137.2, 125.8, 124.4, 120.1, 115.9, 24.7	209 M$^{\cdot+}$ (100)
3	8.71(d,1H), 8.32(d,1H), 7.98(t,1H), 7.50(d,2H), 7.41(s,1H), 7.05(d,1H), 2.42(s,3H, CH$_3$)	150.4, 149.0, 145.5, 138.7, 135.8, 134.7, 134.5, 126.5, 126.4, 123.3, 115.6, 114.8, 21.9	209 M$^{\cdot+}$ (100)
4	8.75(d,1H), 8.33(d,1H), 8.02(t,1H), 7.78(s,1H), 7.55(d,2H), 7.26(t,1H)	150.2, 148.7, 138.4, 125.8, 124.0, 123.0, 122.3, 121.3, 119.4, 114.1, 112.4	231 M$^{\cdot+}$ (100)
5	8.68(d,1H), 8.27(d,1H), 8.11(d,1H), 8.05(d,1H), 7.99(t,1H), 7.53–7.49(m,2H), 7.45(t,1H)	169.7, 154.4, 151.0, 150.6, 138.5, 136.1, 127.3, 126.8, 126.6, 124.0, 123.2, 121.0	212 M$^{\cdot+}$ (100)
6	8.77(d,1H), 8.34(d,1H), 7.89(t,1H), 7.80(d,1H), 7.67(d,1H), 7.46–7.39(m,3H)	161.9, 151.3, 150.4, 146.4, 142.1, 137.2, 126.1, 125.7, 125.0, 123.7, 120.6, 111.3	196 M$^{\cdot+}$ (100)
7	8.79(d,1H), 8.31(d,1H), 8.04(t,1H), 7.70(d,1H), 7.64(s,1H), 7.61(t,1H), 7.29(d,1H), 2.44(s,3H,CH$_3$)	162.1, 150.9, 149.4, 146.0, 142.1, 138.3, 135.2, 128.0, 126.8, 124.2, 120.7, 111.4, 21.7	210 M$^{\cdot+}$ (100)
8	8.78(d,1H), 8.29(d,1H), 8.15(t,1H), 7.72(d,1H), 7.62(s,1H), 7.59(t,1H), 7.25(d,1H), 2.53(s,3H,CH$_3$)	161.5, 151.4, 150.8, 146.1, 139.8, 138.3, 137.1, 127.0, 126.7, 124.0, 120.4, 111.9, 22.0	210 M$^{\cdot+}$ (100)
9	8.93–8.90(dd,2H), 8.24(t,1H), 7,88–7.85(dd,2H), 7.80–7.75(dd,1H), 7.61–7.58(dd,2H)	151.2, 147.8, 142.8, 139.1, 132.6, 128.3, 127.1, 124.8, 115.1	385 M$^{\cdot+}$(5), 349 M$^{\cdot+}$–Cl (10), 312 M$^{\cdot+}$–2Cl (5), 276 M$^{\cdot+}$–3Cl (15), 243 M$^{\cdot+}$–4Cl (5) 195 M$^{\cdot+}$–TiCl$_4$ (100)
10	8.79(d,1H), 8.50(d,1H), 8.08(t,1H), 7.71–7.68(dd,2H), 7.62–7.59(dd,1H), 7.38–7.36(dd,2H)	150.8, 148.9, 144.2, 138.8, 134.3, 127.3, 125.8, 123.9, 115.5	428 M$^{\cdot+}$(2), 392 M$^{\cdot+}$–Cl (15), 355 M$^{\cdot+}$–2Cl (20), 320 M$^{\cdot+}$–3Cl (5), 284 M$^{\cdot+}$–4Cl (5), 195 M$^{\cdot+}$–ZrCl$_4$ (100)
11	n.d.	n.d.	352 M$^{\cdot+}$(5), 316 M$^{\cdot+}$–Cl (20), 281 M$^{\cdot+}$–2Cl (10), 195 M$^{\cdot+}$–VCl$_3$ (100)
12	8.53(d,1H), 8.10–8.06(t,1H), 7.84 (br,2H), 7.61–7.59(d,1H), 7.58–7.56(m,2H), 2.5(s,3H,CH$_3$)	160.5, 148.2, 142.2, 139.5, 133.0, 128.1, 127.0, 122.0, 115.2, 24.8	401 M$^{\cdot+}$(5), 364 M$^{\cdot+}$–Cl (5), 328 M$^{\cdot+}$–2Cl (5), 254 M$^{\cdot+}$–4Cl (5), 209 M$^{\cdot+}$–TiCl$_4$ (100)
13	8.87 (br,1H), 8. 25 (br,1H), 8.02(br,2H), 7.74(br,3H), 2.42(s,3H,CH$_3$)	160.5, 148.1, 142.1, 139.4, 132.7, 128.4, 127.3, 122.5, 115.4, 25.0	442 M$^{\cdot+}$(5), 405 M$^{\cdot+}$–Cl (10), 368 M$^{\cdot+}$–2Cl (10), 329 M$^{\cdot+}$–3Cl (20) 209 M$^{\cdot+}$–ZrCl$_4$ (100)
14	n.d.	n.d.	366 M$^{\cdot+}$(5), 329 M$^{\cdot+}$–Cl (10), 295 M$^{\cdot+}$–2Cl (15), 259 M$^{\cdot+}$–3Cl (20) 209 M$^{\cdot+}$–VCl$_3$ (100)
15	8.86(d,1H), 8.67(d,1H), 8.17(t,1H), 7.70(t,2H), 7.57(s,1H), 7.33(d,1H), 2.47(s,3H,CH$_3$)	151.0, 148.0, 143.7, 139.0, 136.4, 133.9, 131.9, 128.0, 127.7, 124.1, 115.0, 114.5, 22.0	402 M$^{\cdot+}$(5), 364 M$^{\cdot+}$–Cl (5), 328 M$^{\cdot+}$–2Cl(5), 254 M$^{\cdot+}$–4Cl (5), 209 M$^{\cdot+}$–TiCl$_4$ (100)
16	8.84–8.80(m,2H), 8.17(t,1H), 7.71–7.66(m,2H), 7.57(s,1H), 7.34(d,1H), 2.02(s,3H,CH$_3$)	151.1, 147.2, 142.6, 139.0, 137.2, 133.6, 130.5, 128.7, 128.1, 124.6, 114.6, 114.3, 21.9	442 M$^{\cdot+}$(5), 428 M$^{\cdot+}$–CH$_3$ (10), 405 M$^{\cdot+}$–Cl (10), 368 M$^{\cdot+}$–2Cl (10), 329 M$^{\cdot+}$–3Cl (20), 300 M$^{\cdot+}$–4Cl (20) 209 M$^{\cdot+}$–ZrCl$_4$ (100)
17	n.d.	n.d.	366 M$^{\cdot+}$(5), 330 M$^{\cdot+}$–Cl (10), 316 M$^{\cdot+}$–Cl–CH$_3$ (5), 294 M$^{\cdot+}$–2Cl (15), 260 M$^{\cdot+}$–3C l (20), 209 M$^{\cdot+}$–VCl$_3$ (100)
18	8.86(d,1H), 8.70(d,1H), 8.19(t,1H), 7.82(s,1H), 7.77(d,1H), 7.71(t,1H), 7.54–7.50(dd,1H)	150.9, 15.0, 144.2, 139.0, 135.6, 133.6, 130.2, 127.8, 126.4, 124.2, 117.0, 115.1	384 M$^{\cdot+}$–Cl (10), 349 M$^{\cdot+}$–2Cl (7), 229 M$^{\cdot+}$–TiCl$_4$ (50)
19	8.75(d,1H), 8.46(d,1H), 8.04(t,1H), 7.69(d,1H), 7.65(s,1H), 7.58(t,1H), 7.35–7.32(dd,1H)	151.2, 150.5, 146.3, 138.667, 136.0, 132.7, 128.9, 126.8, 125.0, 123.2, 117.2, 115.4	468 M$^{\cdot+}$(10), 426 M$^{\cdot+}$–Cl (40), 387 M$^{\cdot+}$–2Cl (50), 229 M$^{\cdot+}$–ZrCl$_4$ (100)
20	n.d.	n.d.	386 M$^{\cdot+}$(7), 350 M$^{\cdot+}$–Cl (20), 315 M$^{\cdot+}$–2Cl (30), 279 M$^{\cdot+}$–3Cl (5), 229 M$^{\cdot+}$–VCl$_3$ (100)
21	8.70(t,1H), 8.30(d,1H), 8.14(d,1H), 8.07(d,1H), 8.01(t,1H), 7.57(t,2H), 7.53–7.46(m,2H)	169.6, 154.4, 150.9, 150.577, 138.6, 136.1, 127.3, 126.8, 126.7, 124.0, 123.3, 121.1	403 M$^{\cdot+}$(3), 366 M$^{\cdot+}$–Cl (15), 329 M$^{\cdot+}$–2Cl (20), 293 M$^{\cdot+}$–3Cl (10), 212 M$^{\cdot+}$–TiCl$_4$ (100)
22	8.73(t,1H), 8.33(d,1H), 8.18(d,1H), 8.11(d,1H), 8.05(t,1H), 7.60(t,2H), 7.54–7.47(m,2H)	169.7, 154.4, 151.0, 150.7, 138.6, 136.1, 127.4, 126.9, 126.7, 124.0, 123.3, 121.1	445 M$^{\cdot+}$(2), 408 M$^{\cdot+}$–Cl (20), 372 M$^{\cdot+}$–2Cl (10), 300 M$^{\cdot+}$–4Cl (20), 212 M$^{\cdot+}$–ZrCl$_4$ (100)
23	n.d.	n.d.	370 M$^{\cdot+}$(5), 334 M$^{\cdot+}$–Cl (10), 297 M$^{\cdot+}$–2Cl (15), 263 M$^{\cdot+}$–3Cl (5), 212 M$^{\cdot+}$–VCl$_3$ (100)
24	8.75(d,1H), 8.29(d,1H), 8.03(t,1H), 7.81(t,2H), 7.60(t,1H), 7.46–7.37(m,2H)	161.8, 151.1, 150.7, 145.7, 141.8, 138.6, 127.0, 126.9, 125.8, 124.3, 121.0, 112.0	386 M$^{\cdot+}$(2), 245 M$^{\cdot+}$–4Cl (5), 196 M$^{\cdot+}$– TiCl$_4$ (100)
25	8.72(d,1H), 8.26(d,1H), 8.04(t,1H), 7.78(t,2H), 7.57(t,1H), 7.43–7.35(m,2H)	161.9, 151.1, 150.8, 145.8, 141.8, 138.4, 126.9(2C), 125.8, 124.2, 121.0, 111.9	429 M$^{\cdot+}$(2), 392 M$^{\cdot+}$–Cl (50), 356 M$^{\cdot+}$–2Cl (5), 289 M$^{\cdot+}$–4Cl (5), 196 M$^{\cdot+}$– ZrCl$_4$ (100)
26	n.d.	n.d.	353 M$^{\cdot+}$(2), 317 M$^{\cdot+}$–Cl (30), 283 M$^{\cdot+}$–2Cl (5), 196 M$^{\cdot+}$–VCl$_3$ (100)
27	8.77(d,1H), 8.29(d,1H), 8.05(t,1H), 7.69(d,1H), 7.63(s,1H), 7.60(t,1H), 7.28(d,1H), 2.44(s,3H,CH$_3$)	162.0, 150.8, 149.4, 145.9, 142.1, 138.5, 135.3, 128.0, 126.9, 124.2, 120.7, 111.4, 21.7	399 M$^{\cdot+}$(2), 349 M$^{\cdot+}$–Cl–CH$_3$ (5) 325 M$^{\cdot+}$–2Cl (5), 293 M$^{\cdot+}$–3Cl (7), 258 M$^{\cdot+}$–4Cl (5), 210 M$^{\cdot+}$–TiCl$_4$ (100)
28	8.76(d,1H), 8.30(d,1H), 8.05(t,1H), 7.69(d,1H), 7.63(s,1H), 7.61(t,1H), 7.28(d,1H), 2.43(s,3H,CH$_3$)	162.0, 150.8, 149.4, 145.9, 142.1, 138.4, 135.3, 127.9, 126.9, 124.2, 120.7, 111.4, 21.7	443 M$^{\cdot+}$(5), 407 M$^{\cdot+}$–Cl (5), 393 M$^{\cdot+}$–Cl–CH$_3$ (10), 370 M$^{\cdot+}$–2Cl (10), 301 M$^{\cdot+}$–4Cl (5), 210 M$^{\cdot+}$–ZrCl$_4$ (100)
29	n.d.	n.d.	367 M$^{\cdot+}$(5), 331 M$^{\cdot+}$–Cl (10), 316 M$^{\cdot+}$–Cl–CH$_3$ (3), 296 M$^{\cdot+}$–2Cl (5), 210 M$^{\cdot+}$–VCl$_3$ (100)
30	8.80(d,1H), 8.33(d,1H), 8.09(t,1H), 7.72(s,1H), 7.66(d,2H), 7.30(d,1H), 2.45(s,3H,CH$_3$)	161.8, 150.6, 149.4, 145.7, 142.1, 138.8, 135.3, 128.1, 126.9, 124.3, 120.7, 111.4, 21.7	400 M$^{\cdot+}$(3), 349 M$^{\cdot+}$–Cl–CH$_3$ (5) 325 M$^{\cdot+}$–2Cl (5), 293 M$^{\cdot+}$–3Cl (10), 258 M$^{\cdot+}$–4Cl (10), 210 M$^{\cdot+}$–TiCl$_4$ (100)

(*continued on next page*)

Table 4 (*continued*)

Compound no.	^{1}H NMR δ [ppm]	^{13}C NMR δ [ppm]	Mass m/z (%)
31	8.80(d,1H), 8.34(d,1H), 8.08(t,1H), 7.73(s,1H), 7.67(d,2H), 7.31(d,1H), 2.46(s,3H,CH_3)	161.9, 150.7, 149.4, 145.8, 142.1, 138.6, 135.3, 128.1, 126.9, 124.3, 120.8, 111.4, 21.7	443 $M^{\cdot+}$(2), 407 $M^{\cdot+}-Cl$ (7), 393 $M^{\cdot+}-Cl-CH_3$ (5), 370 $M^{\cdot+}-2Cl$ (10), 301 $M^{\cdot+}-4Cl$ (5), 210 $M^{\cdot+}-ZrCl_4$ (100)
32	n.d.	n.d.	367 $M^{\cdot+}$(3), 331 $M^{\cdot+}-Cl$ (5), 317 $M^{\cdot+}-Cl-CH_3$ (3), 296 $M^{\cdot+}-2Cl$ (5), 210 $M^{\cdot+}-VCl_3$ (100)

4. Conclusions

2-(Benzimidazolyl, benzothiazolyl, and benzoxazolyl) pyridines form dissymmetric chelate complexes with Ti, Zr and V chlorides. After activation with MAO the generated catalysts polymerize ethylene in solution with various activities. Structure–property-relationships indicate that the nature of the metal, the nature and position of substituents and the hetero atoms determine the performance of such catalysts. The highest activity (1154.8 kg PE/mol cat h) was obtained with the vanadium catalyst **29**/MAO containing a benzoxazolyl moiety and a methyl substituent at the meta position of the phenylidene ring. The high molecular weights of the produced polymers (**12**/MAO, 1.76×10^6 g/mol) indicate low energy barriers for the olefin insertion and high barriers for the termination steps. Relative broad molecular weight distributions of the produced polyethylenes (PD = 4.4–5.7) could result from the existence of several active sites in the polymerization process.

Acknowledgements

We thank SABIC company (Riyadh, Saudi Arabia) for the financial support and the GPC measurements and University of Juba (Khartoum, Sudan) for the financial support of H.A.E. for the first year.

References

[1] H.A. Elagab, H.G. Alt, Inorg. Chim. Acta 428 (2015) 100.
[2] H.A. Elagab, H.G. Alt, JJC (in press).
[3] R. Breslow, J.T. Hunt, R. Smiley, T. Tamowski, J. Am. Chem. Soc. 105 (1983) 5337.
[4] R.H. Beer, W.B. Tolmann, S.G. Bott, S. Lippard, J. Inorg. Chem. 28 (1989) 4557.
[5] C. Kimplin, W.E. Allen, G. Parkin, J. Chem. Soc., Chem. Commun. (1995) 1813.
[6] J. Chatlas, S. Kaizaki, E. Kita, P. Kita, N. Sakagami, R. van Eldik, J. Chem. Soc., Dalton Trans. (1991) 91.
[7] J.A. Winter, D. Caruso, R.E. Shepherd, Inorg. Chem. 27 (1988) 1086.
[8] G. Jin, F. Chen, CN 101089022 (2007).
[9] A.E. Ceniceros-Gomez, N. Barba-Behrensa, M.E. Quiroz-Castro, S. Bernes, H. Nöth, S.E. Castillo-Blum, Polyhedron 19 (2000) 1821.
[10] A.S. Salameh, H.A. Tayim, Polyhedron 6 (1982) 543.
[11] M. Mitani, J. Mohri, Y. Yoshida, J. Saito, S. Ishaii, K. Tsuru, S. Matsui, R. Furuyama, T. Nakano, H. Tanaka, S. Kojoh, J. Matsugi, N. Kashima, T. Fujita, J. Am. Chem. Soc. 124 (2002) 3327.
[12] V. Volkis, E. Nelkenbaum, A. Lisovskii, G. Hasson, R. Semiat, M. Kapon, M. Botoshansky, Y. Eishen, M.S. Eisen, J. Am. Chem. Soc. 125 (2003) 2179.
[13] Y. Yoshida, J. Mohri, S. Ishii, M. Mitani, J. Saito, S. Matsui, H. Makio, T. Nakano, H. Tanaka, M. Onda, Y. Yamamoto, A. Mizuno, T. Fujita, J. Am. Chem. Soc. 126 (2004) 12023.
[14] C. Redshaw, Y. Tang, Chem. Soc. Rev. 41 (2012) 4484.
[15] M.C. Baier, M.A. Zuideveld, S. Mecking, Angew. Chem., Int. Ed. 53 (2014) 9722.
[16] A.C. Gottfried, M. Brookhart, Macromolecules 36 (2003) 3085.
[17] S.A. Svejda, M. Brookhart, Organometallics 18 (1999) 65.
[18] C. Rai, J.B. Braunwarth, J. Org. Chem. 26 (1961) 3434.
[19] R.L. Schriner, R.W. Upson, J. Am. Chem. Soc. 63 (1941) 2277.
[20] M.A. Phillips, J. Chem. Soc. (1928) 2393.
[21] M. Bochmann, L.M. Wilson, J. Chem. Soc., Chem. Commun. 21 (1986) 1610.
[22] R.F. Jordan, C.S. Bajgur, W.E. Dasher, A.L. Rheingold, Organometallics 6 (1987) 1041.
[23] M. Seitz, W. Milius, H.G. Alt, J. Mol. Catal. A 261 (2007) 246.
[24] A.C. Möller, R. Blom, R.H. Heyn, O. Swang, J. Kopf, T. Seraidaris, J. Chem. Soc., Dalton Trans. (2006) 2098.
[25] A.C. Möller, R. Blom, O. Swang, A. Hannisdal, E. Rytter, J.A. Stovneng, T. Piel, J. Phys. Chem. 112 (2008) 4074.
[26] H.A. Elagab, H.G. Alt, Polymer (submitted).
[27] L.E. Manzer, Inorg. Synth. 21 (1982) 135.

Please cite this article in press as: H.A. Elagab, H.G. Alt, Inorg. Chim. Acta (2015), http://dx.doi.org/10.1016/j.ica.2015.03.021